Research Article

Clinically Actionable Insights into Initial and Matched Recurrent Glioblastomas to Inform Novel Treatment Approaches

H. P. Ellis,[1] C. E. McInerney,[2] D. Schrimpf,[3] F. Sahm,[3] A. Stupnikov,[2,4] M. Wadsley,[5] C. Wragg,[5] P. White (ID)**,[6] K. M. Prise,[2] D. G. McArt** (ID)**,[2] and K. M. Kurian** (ID)**[1]**

[1]*Brain Tumour Research Centre, University of Bristol, Bristol, UK*
[2]*Centre for Cancer Research and Cell Biology, Queen's University, Belfast, UK*
[3]*Department of Neuropathology, Institute of Pathology, Ruprecht-Karls-University Heidelberg, Heidelberg, Germany*
[4]*Department of Oncology, School of Medicine, Johns Hopkins University, Baltimore, MD 21287, USA*
[5]*Bristol Genetics Laboratory, North Bristol NHS Trust, Bristol, UK*
[6]*Applied Statistics Group, University of the West of England, Bristol, UK*

Correspondence should be addressed to D. G. McArt; d.mcart@qub.ac.uk and K. M. Kurian; kathreena.kurian@bristol.ac.uk

H. P. Ellis and C. E. McInerney contributed equally to this work.

Glioblastoma is the most common primary adult brain tumour, and despite optimal treatment, the median survival is 12–15 months. Patients with matched recurrent glioblastomas were investigated to try to find actionable mutations. Tumours were profiled using a validated DNA-based gene panel. Copy number variations (CNVs) and single nucleotide variants (SNVs) were examined, and potentially pathogenic variants and clinically actionable mutations were identified. The results revealed that glioblastomas were IDH-wildtype (IDH^{WT}; $n = 38$) and IDH-mutant (IDH^{MUT}; $n = 3$). SNVs in $TSC2$, $MSH6$, $TP53$, $CREBBP$, and $IDH1$ were variants of unknown significance (VUS) that were predicted to be pathogenic in both subtypes. IDH^{WT} tumours had SNVs that impacted RTK/Ras/PI(3)K, p53, WNT, SHH, NOTCH, Rb, and G-protein pathways. Many tumours had $BRCA1/2$ (18%) variants, including confirmed somatic mutations in haemangioblastoma. IDH^{WT} recurrent tumours had fewer pathways impacted (RTK/Ras/PI(3)K, p53, WNT, and G-protein) and CNV gains ($BRCA2$, $GNAS$, and $EGFR$) and losses ($TERT$ and $SMARCA4$). IDH^{MUT} tumours had SNVs that impacted RTK/Ras/PI(3)K, p53, and WNT pathways. VUS in $KLK1$ was possibly pathogenic in IDH^{MUT}. Recurrent tumours also had fewer pathways (p53, WNT, and G-protein) impacted by genetic alterations. Public datasets (TCGA and GDC) confirmed the clinical significance of findings in both subtypes. Overall in this cohort, potentially actionable variation was most often identified in $EGFR$, $PTEN$, $BRCA1/2$, and ATM. This study underlines the need for detailed molecular profiling to identify individual GBM patients who may be eligible for novel treatment approaches. This information is also crucial for patient recruitment to clinical trials.

1. Introduction

Gliomas are the largest group of intrinsic brain tumours with age adjusted incidence rates ranging from 4.67 to 5.73 per 100,000, causing more years of life lost compared with other cancers [1, 2]. Glioblastoma (GBM) is the most malignant glioma and is classified molecularly as IDH-wildtype and IDH-mutant GBM [3–10]. During gliomagenesis, an array of genetic alterations may cause the dysregulation of cell growth signalling and cell cycle pathways [6, 11–15]. In particular, mutations in $RTKs$ (receptor tyrosine kinases) and/or loss of $PTEN$ (phosphatase and tensin homolog) alter the $PI3K$ (phospinositide 3-kinase)/AKT cell growth pathway [11]. Further mutations in $CDKN2A$ or $CDK4$ (cyclin-dependent kinase) lead to uncontrolled progression of the cell cycle, as do mutations in $TP53$ [16]. Neural stem cells in the subventricular zone may harbour recurrent driver somatic mutations that are shared with the tumour bulk (e.g., $P53$, $PTEN$, $EGFR$, and $TERT$) [17]. Telomerase (reactivation or reexpression) can occur in IDH wildtype and mutant

GBMs driven either by telomerase reverse transcriptase (*TERT*) promoter mutations or other mechanisms [8, 18]. The current standard-of-care for glioblastomas remains as maximal safe surgical resection with concurrent radiotherapy and temozolomide (TMZ) chemotherapy (Stupp protocol) [19, 20]. Personalised therapies remain promising although trials have been unsuccessful to date [21–23]. For example, dysregulated *PI3K* and *RTKs* (*EGFR*, *MET*, *PDGFR*, *FGFR*, and *BRAF*) genes have been targeted with various small molecules, antibodies, and inhibitors [24–29]. To date, entry to clinical trials for GBM has not been based on a detailed molecular analysis of an individual patient's tumour using high throughput sequencing (HTS). HTS-based molecular diagnostics can aid the detection of genetic alterations, information required for personalised medicine [30, 31]. Herein, initial and matched recurrent glioblastomas were examined using HTS with a validated DNA-based diagnostic panel. Potentially pathogenic variants and clinically actionable mutations were identified in different GBM subtypes. Findings were validated using TCGA-GBM and GDC datasets.

2. Materials and Methods

2.1. Clinical Specimens. Ethical approval was given by Brain Tumour Bank South West and Brain UK (Ref: 14/010). All patients had been treated using the Stupp protocol [19]. A total of 72 formalin-fixed paraffin-embedded (FFPE) samples from 54 patients were identified (2009–2014). Only FFPE slides with >30% tumour cells available for macrodissection were selected. Samples lacking cellularity or excessively necrotic were excluded. Following quality control, 67 samples for 46 patients and 19 with matched recurrent samples available were identified. Of these, a total of 49 samples were successfully sequenced for 41 patients (21 males; 20 females; mean age 55 years, range 16–78 years; see Tables 1 and S1). Matched initial and recurrent tissue samples were analysed for 8 patients (2 males; 6 females). Recurrent tumours all occurred locally to the initial tumour. Anonymised patient cases in the GBM cohort were numbered 1–11, 16–41, and 43–46, and "*a*" and "*b*" indicated initial and recurrent tumour samples, respectively (Table S1).

2.2. HTS Neuro-Oncology Gene Panel. A published HTS DNA-based panel that uses targeted enrichment to examine exonic, selected intronic and promoter regions of 130 clinically relevant neuro-oncology genes was utilised (see Table S2) [30]. The diagnostic panel has been optimised for use either with fresh-frozen or FFPE tissue. Validation studies of the HTS panel analysing ~200 single nucleotide variants (SNVs), gene fusions, and copy number variants (CNVs) showed 98% concordance with single marker tests [30]. Using the HTS panel, genetic alterations in tumours were characterized, and *TERT* promoter and *IDH1/2* status confirmed.

2.3. DNA Extraction, HTS Library Preparation, Sequencing, and Analysis. Slides were deparaffinised and rehydrated using xylene and ethanol and left to dry. Tissue sections were

Table 1: Summary of the clinical data for patients genomically profiled in this study ($n = 41$). Patients with *IDH*-wildtype and *IDH*-mutant glioblastoma tumours were identified from the BRASH clinical database between 2009 and 2014.

Characteristic	*IDH*-wildtype	*IDH*-mutant
Number of patients	38	3
Age		
Mean	54	42
Median (range)	52 (16–78)	50 (19–58)
Gender		
Male	19 (50%)	2 (66%)
Female	20 (50%)	1 (33%)
Survival range (months)	2–48	5–12
Tumour location		
Temporal lobe	8 (21%)	2 (66%)
Frontal lobe	15 (39%)	
Parietal lobe	4 (11%)	
Occipital	4 (11%)	
More than one lobe	5 (13%)	1 (33%)
Multifocal	1 (3%)	
No data	1 (3%)	
Tumour recurrence		
Initial	38	3
Recurrent	7	1

then microdissected and placed into 180 uL ATL buffer. DNA was extracted from tissue sections ($10 \times 10 \, \mu m$) according to manufacturer's instructions using the QIAamp DNA FFPE Tissue Kit (Qiagen, Manchester, UK). Following assessment of DNA quality and quantity, libraries were prepared using 200 ng of genomic DNA with an optical density 260/280 ratio between 1.8 and 2.0. Libraries were constructed using the SureSelect^{XT} Target Enrichment System for Illumina Paired-End Multiplexed Sequencing Library protocol (Agilent). PCR master mixes were prepared using the SureSelect^{XT} Library Prep Kit ILM following manufacturer's guidelines. In accordance with Illumina guidelines, libraries with a concentration of 4 nM were diluted to 20 pM, denatured, and sequenced on a NextSeq 500 (Illumina). HTS data were analysed following the pipeline described by Sahm et al. [30]. In brief, raw reads were demultiplexed, converted to *fastq*, quality checked, and manually trimmed when necessary. Paired-end reads were aligned to the human genome (version GRch37; hg19), and duplicate sequences were removed.

2.4. CNV Analysis in the GBM Cohort. CNVs were investigated using a coverage analysis. The ratio of on- and off-target reads, coverage per target region, and mean coverage per sample were estimated using the *R* package *TEQC* [32]. Measures provided an estimate of read depth, as the number of reconstructed strands across a region of interest, and this was utilised for CNV estimation of genes. Data normalisation and CNV comparison to a reference control were made using the *R* package *seqCNA* [33]. This method has previously been validated with 100% concordance for 47 GBM cases using 450 k data [30]. Potential CNV gain or loss is indicated by deviations from a proportional read depth of 50%, considered a normal gene copy number.

2.5. SNV Analysis in the GBM Cohort. Variant calling followed a modified pipeline, as described by Sahm et al. [30]. In brief, variants were called using *SAMtools mpileup* [34]. Variant calls were then filtered by (a) read depth ≥ 40, (b) genotype quality ≥ 99, (c) minimum allele frequency set at 10, and (d) at least 10% read coverage from each strand using the *R* package *VariantAnnotation* [35]. *TERT* promoter position calls were not filtered due to their low detection rate because of difficulties with their amplification as a GC-rich region [30]. Nonsynonymous filtered variants were annotated with the most up to date information including dbSNP and COSMIC identifiers using the online tool *wANNOVAR* [36]. Matched normal tissue was unavailable for comparison for the identification of germline mutations. Thus, to try to discern pathogenic from benign variants, the frequency of a variant in the general population was used as a key criterion in their clinical interpretation to try to exclude germline mutations. SNVs were filtered to those with a frequency of ≥0.01 in the 1,000 Genomes database and ≥0.05 in the Genome Aggregation Database (gnomAD), previously known as the Exome Aggregation Consortium database. gnomAD warehouses whole genome sequences from 15,496 unrelated individuals [37]. As the ethnicity of patients in the GBM cohort was unknown, SNV frequencies were compared to overall frequencies (rather than regional) of both databases. Filtered SNVs impacting genes were categorised into biological pathways using *GeneCards* [38]. SNVs occurring in the potentially clinically actionable genes: *EGFR, PTEN, CDKN2A, RB1, TP53, ATM, ATR, MSH6, PDGFRA, PIK3CA, PIK3R1, SMO, PTCH1, BRCA1, BRCA2,* and *BRAF*, were quantified in the initial and matched recurrent tumours. Further filtering was applied to SNV results to try to identify variants of unknown significance (VUS) that are possibly pathogenic and underpin gliomagenesis. VUS considered to be possibly pathogenic, were those that had no frequency recorded in the 1,000 Genomes database, and were predicted to be damaging by both *LJB SIFT* and *FATHMM-MKL* software [39]. All genomic positions listed for SNVs identified by this study are from the human genome version GRch37.

2.6. VUS and CNV Analysis in the TCGA-GBM and GDC Datasets. VUS identified as possibly pathogenic mutations in the GBM cohort were further investigated for supporting evidence of their clinical significance using TCGA-GBM and GDC datasets. Frequencies of cases with mutations in genes were investigated in the GDC data portal. Abundance of mutations and copy number alterations within the TCGA-GBM dataset was visualised as an oncoprint plot generated using *GlioVis*, a data visualisation tool for brain tumour datasets [40].

2.7. Survival Analyses of IDH-Wildtype Glioblastomas. A Cox proportional hazard regression analysis was implemented to determine the relationship between the total number of SNVs (median split) and overall survival. *MGMT* methylated and unmethylated GBMs were investigated separately. Survival analyses and plotting of results as

Kaplan–Meier graphs were carried out using *R* software [41]. Of the 41 patients, univariate survival analysis was carried out on the 33 *IDH*-wildtype patients only. Omitted patients included the three *IDH*$^{\text{MUT}}$ patients and a further five patients lacking survival information.

3. Results

3.1. Overview of Genomic Profiling of Glioblastoma Tumours and IDH Status. In all, 49 samples from 41 patients including 8 matched samples were genomically profiled (Tables 1 and S1). Results could not be obtained for 5 initial and 13 recurrent samples from 11 patients, giving a sequencing failure rate of ~22%. SNVs were not identified in 5 samples (9%). Recurrent tumour samples were necrotic with low cellularity, which probably impacted DNA quality and sequencing success. Majority of tumours were *IDH*-wildtype (38/41; 93%) with the exception of three cases (8, 35, and 39) that were *IDH*-mutant (Table S1). Cases 8, 35, and 39 had a C to T mutation located at the *IDH1* diagnostic hotspot R132 (Chr2: 209113112; GRCh37). Only one other case (6a) had an *IDH1* mutation located at Chr2: 209108284 (GRCh37). This mutation was 4,828 bp upstream of the diagnostic hotspot (R132); hence, case 6a was considered *IDH*-wildtype. One case had an *IDH2* mutation (Chr15: 90627553); however, this did not coincide with known somatic mutations located at 15q26.1 codons R140 (Chr15: 90631934) and R172 (Chr15: 90631837). *TERT* mutations were observed in *IDH* wildtype initial (Chr5: 1254594; Chr5: 1294166) and recurrent tumours (Chr5: 1,254,594); however, none coincided with known somatic mutations in promoter regions at the C228 (Chr5: 1,295,228) and C250 loci (Chr5: 1,295,250; hg19).

3.2. SNVs Detected in Initial and Recurrent IDH$^{\text{WT}}$ Glioblastomas. A total of 134 nonsynonymous and three stop-gain SNVs were detected from initial ($n = 125$; Table S4) and recurrent *IDH*$^{\text{WT}}$ tumours ($n = 12$; Table S5). Including *IDH*1/2 mutations, SNVs affected 52 genes across nine biological pathways during the different phases of gliomagenesis (Figures 1 and 2; Tables 2 and 3). Majority of initial tumours had SNVs in a gene in the RTK/Ras/PI(3)K pathways (79%; 30/38) followed by the p53 DNA damage repair pathway (61%; 23/38). Two stop-gain SNVs were identified from the p53 genes *MSH2* (Chr2: 47705428; rs63751155) and *TP53* (Chr17: 7579315; COSM326717; COSM3388232; COSM326718; COSM3388233; COSM326716) in initial tumours; both variants were predicted to be pathogenic by *FATHMM-MKL* (Table S4). A large proportion of initial *IDH*$^{\text{WT}}$ tumours had SNVs in the p53 pathway genes *BRCA1* (18%; 7/38) and *BRCA2* (18%; 7/38; Table 4). Six *BRCA1* variants were detected including a confirmed somatic mutation in adenocarcinoma (COSM6612515; Chr17: 41244952) [42]. Six *BRCA2* variants were detected including confirmed somatic mutations in haemangioblastoma (COSM3753648, Chr13: 32914236; COSM5019704, Chr13: 32953549) [43]. Over half of initial *IDH*$^{\text{WT}}$ tumours had an SNV in a WNT signalling pathway gene (58%; 22/38).
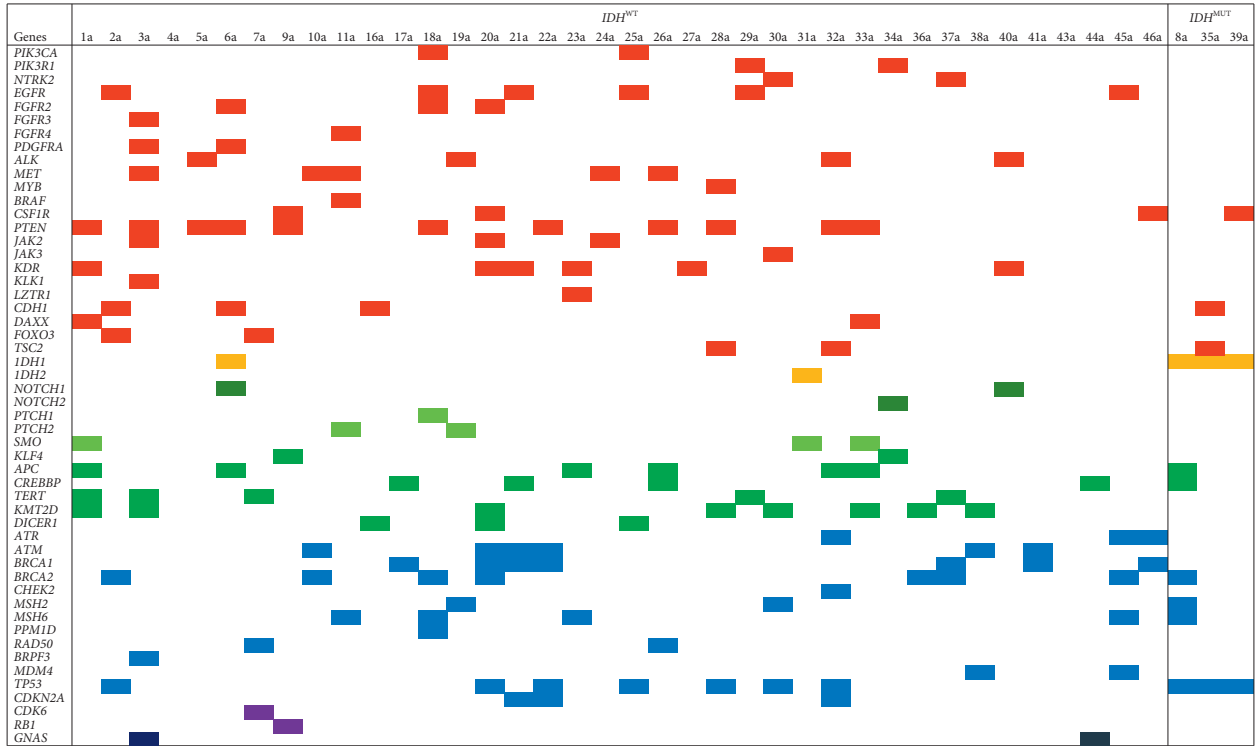
Figure 1: Summary of the genes identified with SNVs in IDH^{WT} ($n = 38$) and IDH^{MUT} diffuse tumours ($n = 3$; cases 8a, 35a, and 39a). Genes are arranged hierarchically within their pathways for the RTK/Ras/PI(3)K (red), IDH (yellow), NOTCH, SHH, and WNT signalling (variations of green), p53 (blue), Rb (purple), and G-proteins (dark blue) pathways. Numbers across the top axis denote the patient identifier.

Figure 2: Summary of the genes identified with SNVs in matched initial and recurrent IDH^{WT} ($n = 7$) and IDH^{MUT} diffuse tumours ($n = 1$; case 8). Genes are arranged hierarchically within their pathways for the RTK/Ras/PI(3)K (red), IDH (yellow), NOTCH, SHH, and WNT signalling (variations of green), p53 (blue), Rb (purple), and G-proteins (dark blue) pathway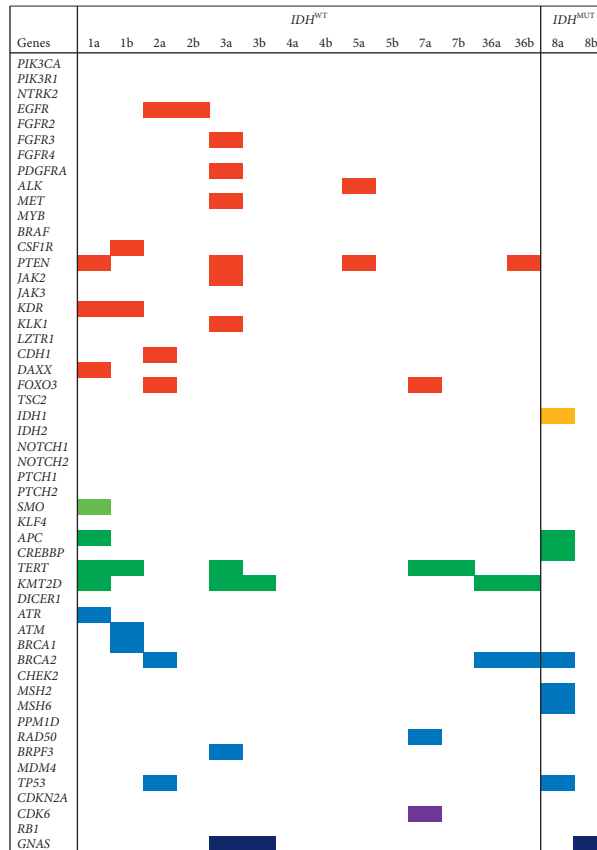s. Numbers across the top axis denote the patient identifier; "a" and "b" indicate initial and recurrent tumours, respectively.

Table 2: Summary of the number and proportion of *IDH*-wildtype and *IDH*-mutant glioblastoma patients with SNVs in genes in the RTK/Ras/PI(3)K, p53 DNA damage repair, WNT signalling, SHH, NOTCH, Rb, and G-protein pathways.

Pathway	*IDH*-wildtype				*IDH*-mutant			
	Initial		Recurrent		Initial		Recurrent	
	%	N	%	N	%	N	%	N
RTK/Ras/PI(3)K	79	30/38	43	3/7	66	2/3	0	0/1
p53 DNA damage repair	61	23/38	29	2/7	100	3/3	100	1/1
WNT signalling	58	22/38	57	4/7	33	1/3	100	1/1
SHH	16	6/38	0	0/7	0	0/3	0	0/1
NOTCH	8	3/38	0	0/7	0	0/3	0	0/1
Rb	5	2/38	0	0/7	0	0/3	0	0/1
G-protein	5	2/38	14	1/7	0	0/3	100	1/1

Multiple variants (*n*) were detected for the WNT genes *KMT2D/MLL2* (*7*), *CREBBP* (*4*), *DICER1* (*3*), *APC* (*3*), *TERT* (*2*), and *KLF4* (*2*). IDH^{WT} tumours also showed variation in SHH (16%; 6/38) and NOTCH (8%; 3/38) pathways. A small proportion of initial tumours had SNVs in the G-protein gene, *GNAS* (5%; 2/38), *IDH1/2* (5%; 2/38), and the Rb-specific cell-cycle regulation genes *CDK6* and *RB1* (5%; 2/38). The *RB1* variant was a stop-gain SNV (Chr13: 48953735), but it was not pathogenic. Among IDH^{WT} tumours, 40 SNVs in 21 genes were VUS that were predicted to be functionally damaging (Tables 3 and S3). Potentially pathogenic VUS impacted *IDH1* and genes in the p53 (*ATM*, *BRCA1*, *CHEK2*, *MSH6*, *PPM1D*, and *TP53*), RTK/Ras/PI(3)K (*BRAF*, *DAXX*, *EGFR*, *FGFR2*, *JAK2*, *MYB*, *PIK3CA*, *PIK3R1*, *TSC2*, and *PTEN*), SHH (*PTCH1* and *SMO*), and WNT pathways (*CREBBP*). Two-thirds of initial IDH^{WT} tumours (63%; 24/38) harboured potentially actionable variation most frequently in *PTEN* (29%; 11/38), followed by *BRCA1* (18%; 7/38), *BRCA2* (18%; 7/38), *TP53* (18%; 7/38), *EGFR* (16%; 6/38), *ATM* (16%; 6/38), and *ATR* (8%; 3/38; see Table 4). Recurrent IDH^{WT} tumours had SNVs in genes in the RTK/Ras/PI(3)K (43%; 3/7), WNT signalling (57%; 4/7), and p53 pathways (29%) in the genes *BRCA1* (14%; 1/7) and *BRCA2* (14%; 1/7) and *GNAS* (14%; 1/7). IDH^{WT} recurrent tumours were not mutated in NOTCH, SHH, Rb, or *IDH* genes (Figure 2 and Table S5). In the matched initial tumour, 16 genes showed variation, four of which were also mutated in the recurrent tumour. An additional three SNVs were recorded only in the recurrent tumour in *CSF1R*, *ATM*, and *BRCA1*. Possibly pathogenic VUS were identified in *PTEN* in recurrent IDH^{WT} tumours. Almost half of recurrent IDH^{WT} tumours (43%; 3/7) harboured at least one potentially actionable variation in the genes *EGFR* (14%; 1/7), *PTEN* (14%; 1/7), *BRCA1* (14%; 1/7), *BRCA2* (14%; 1/7), and *ATM* (14%; 1/7; Figure 2 and Table 4).

3.3. SNVs Detected in Initial and Recurrent IDH^{MUT} Glioblastomas.

SNVs detected in IDH^{MUT} initial (*n* = 12) and recurrent tumours (*n* = 1; Tables S4, and S5) impacted *IDH1* and 10 genes across 5 biological pathways (Figures 1 and 2; Table 2). Majority of initial tumours had SNVs in genes in the RTK/Ras/PI(3)K (66%; 2/3), followed by p53 (100%; 3/3) and WNT signalling pathway (33%; 1/3). All initial IDH^{MUT} tumours (100%; 3/3) harboured at least one potentially actionable variation in *TP53* (100%; 3/3), *BRCA2*

(33%; 1/3), and *MSH6* (33%; 1/3; Table 4). Just 7 SNVs in 6 genes were VUS that were possibly pathogenic in IDH^{MUT} initial tumours. These included *IDH1* and the p53 pathway genes *MSH6* and *TP53* and the RTK/Ras/PI(3)K genes *KLK1* and *TSC2* and the *CREBBP* gene in the WNT pathway (Table 3). The *KLK1* variant was potentially pathogenic in IDH^{MUT} but not in IDH^{WT}. The recurrent IDH^{MUT} tumour had SNVs in p53, WNT signalling, and G-protein pathway genes. Matched analysis revealed that seven genes had SNVs in the initial that were not observed in the recurrent tumour (Figure 2). The recurrent tumour had SNVs in one gene not recorded in the initial (*GNAS*). No genes had SNVs that were potentially actionable in the recurrent IDH^{MUT} tumour (Table 4).

3.4. CNVs in IDH^{WT} and IDH^{MUT} Glioblastomas.

CNVs were detected in IDH^{WT} tumours only (Table S6). The results for CNVs in the corresponding genes in TCGA-GBM are presented in Figure S1. For sample 36, there appears to be a hemizygous deletion in *BRCA2* in the initial, but a CNV gain in the recurrent tumour. Both trends were identified in TCGA-GBM, but predominantly *BRCA2* had shallow deletions. There were CNV gains in *GNAS* for recurrent sample *3b*. TCGA-GBM results also predominantly indicate CNV gains for *GNAS*. In recurrent samples *1b* and *7b*, *TERT* appeared to have hemizygous deletions. TCGA-GBM had both *TERT* CNV losses and gains with no predominant trend evident. For *SMARCA4*, there appears to be a CNV gain in initial sample *1* but a hemizygous deletion in the recurrent sample. TCGA-GBM had mostly CNV gains with some losses for *SMARCA4*. Significant CNV gains in *EGFR* were observed for initial and recurrent sample *2* and similarly in TCGA-GBM cases.

3.5. Investigation of the Corresponding Genes (with Mutations and CNVs in the GBM Cohort) in the TCGA-GBM and GDC Datasets.

The results of investigations in the TCGA-GBM and GDC datasets for the 21 genes identified with VUS that were possibly pathogenic in the GBM cohort are presented in Figure S2. A summary of SNVs identified from those corresponding genes in the TCGA-GBM dataset is provided in Table S7. TCGA-GBM cases in the mutation data included 6 verified and 2 ambiguous *IDH*-mutant individuals; however, majority of cases are unannotated. *PTEN* was the

TABLE 3: Comparison of genes with SNVs identified in *IDH*-wildtype and *IDH*-mutant initial and recurrent tumours in the GBM cohort with those outlined by Barthel et al. [8], described for the five phases of gliomagenesis.

Gliomagenesis phases	Pathway	Common tumour genetic alterations (Barthel et al.)	IDH wildtype				IDH-mutant				Diagnostic panel (Y/N)
			Barthel et al.	GB-initial	GB-recurrent	GB-potentially pathogenic VUS	Barthel et al.	GB-initial	GB-recurrent	GB-potentially pathogenic VUS	
I: initial growth	IDH		—	*IDH1*	—	Y	*IDH1*	*IDH1*	—	Y	Y
	IDH		—	*IDH2*	—		*IDH2*	—	—		Y
	Rb		*CDK6*	*CDK6*	—		—	—	—		Y
	RTK/Ras/PI(3)K		*EGFR*	*EGFR*	*EGFR*	Y	—	—	—		Y
	RTK/Ras/PI(3)K		*MET*	*MET*	—		—	—	—		Y
	RTK/Ras/PI(3)K		*PDGFRA*	*PDGFRA*	—		*PDGFRA*	—	—		Y
	RTK/Ras/PI(3)K		*PIK3CA*	*PIK3CA*	—	Y	—	—	—		Y
	RTK/Ras/PI(3)K		*PIK3R1*	*PIK3R1*	—	Y	—	—	—		Y
	RTK/Ras/PI(3)K		*PTEN*	*PTEN*	*PTEN*	Y	—	—	—		Y
	WNT		*TERT*	*TERT*	*TERT*		—	—	—		Y
			NF1	—	—		—	—	—		Y
							CTCF				N
			TET1								N
II: oncogene-induced senescence	p53	*TP53*	*TP53*	*TP53*	—	Y	*TP53*	*TP53*	—	Y	Y
	p53	*CDKN2A*	*CDKN2A*	*CDKN2A*	—		—	—	—		Y
	p53	*PPM1D*	*PPM1D*	*PPM1D*	—	Y	—	—	—		Y
	Rb	*RB1*		*RB1*	—		—	—	—		Y
	RTK/Ras/PI(3)K	*BRAF*		*BRAF*	—	Y	—	—	—		Y
		CDKN2B	*CDKN2B*	—	—		—	—	—		Y
		ACVR1	—	—			—	—	—		Y
III: stressed growth	p53	*ATM*		*ATM*	*ATM*	Y					Y
	p53	*ATR*		*ATR*	—	Y					Y
		MYC		—	—						Y
		CDK4		—	—						Y
		MDM2		—	—						Y
IV: replicative senescence/crisis		*CHD5*									N
		TREX1									N
							Terra				N
		RB1	—	*RB1*	—		—	—	—		Y
	WNT	*TERT*	*TERT*	*TERT*	*TERT*		—	—	—		Y
	p53	*TP53*	*TP53*	*TP53*	—	Y	*TP53*	*TP53*	—	Y	Y
		ATRX	-	—			*ATRX*	—	—		Y
			—	*DAXX*	—	Y	*DAXX*	—	—		Y
V: immortalisation and dedifferentiation		*OLIG2*									N
		SOX2									N

TABLE 3: Continued.

Gliomagenesis phases	Pathway	Common tumour genetic alterations (Barthel et al.)	IDH wildtype				IDH-mutant				Diagnostic panel (Y/N)
			Barthel et al.	GB-initial	GB-recurrent	GB-potentially pathogenic VUS	Barthel et al.	GB-initial	GB-recurrent	GB-potentially pathogenic VUS	
GB-SNVs	G-proteins		—	GNAS	GNAS		—	—	GNAS		Y
	NOTCH		—	NOTCH1	—		—	—	—		Y
	NOTCH		—	NOTCH2	—		—	—	—		Y
	p53		—	BRCA1	BRCA1	Y	—	—	—		Y
	p53		—	BRCA2	BRCA2		—	BRCA2	—		Y
	p53		—	BRPF3	—		—	—	—		Y
	p53		—	MDM4	—		—	—	—		Y
	p53		—	MSH2	—		—	MSH2	—		Y
	p53		—	MSH6	—	Y	—	MSH6	—	Y	Y
	p53		—	RAD50	—		—	—	—		Y
	RTK/Ras/PI(3)K		—	ALK	—		—	—	—		Y
	RTK/Ras/PI(3)K		—	CDH1	—		—	CDH1	—		Y
	RTK/Ras/PI(3)K		—	CSF1R	CSF1R		—	CSF1R	—		Y
	RTK/Ras/PI(3)K		—	FGFR2	—	Y	—	—	—		Y
	RTK/Ras/PI(3)K		—	FGFR3	—		—	—	—		Y
	RTK/Ras/PI(3)K		—	FGFR4	—		—	—	—		Y
	RTK/Ras/PI(3)K		—	FOXO3	—		—	—	—		Y
	RTK/Ras/PI(3)K		—	JAK2	—	Y	—	—	—		Y
	RTK/Ras/PI(3)K		—	KDR	KDR		—	—	—		Y
	RTK/Ras/PI(3)K		—	KLK1	—		—	KLK1	—	Y	Y
	RTK/Ras/PI(3)K		—	LZTR1	—		—	—	—		Y
	RTK/Ras/PI(3)K		—	MYB	—	Y	—	—	—		Y
	RTK/Ras/PI(3)K		—	NTRK2	—		—	—	—		Y
	RTK/Ras/PI(3)K		—	TSC2	—	Y	—	TSC2	—	Y	Y
	SHH		—	PTCH1	—	Y	—	—	—		Y
	SHH		—	PTCH2	—		—	—	—		Y
	SHH		—	SMO	—	Y	—	—	—		Y
	WNT		—	APC	—		—	APC	—		Y
	WNT		—	CREBBP	—	Y	—	CREBBP	—	Y	Y
	WNT		—	DICER1	—		—	—	—		Y
	WNT		—	KLF4	—		—	—	—		Y
	WNT		—	KMT2D	—		—	—	—		Y

TABLE 3: Continued.

Gliomagenesis phases	Pathway	Common tumour genetic alterations (Barthel et al.)	IDH wildtype				IDH-mutant				Diagnostic panel (Y/N)
			Barthel et al.	GB-initial	GB-recurrent	GB-potentially pathogenic VUS	Barthel et al.	GB-initial	GB-recurrent	GB-potentially pathogenic VUS	
Risk mutations related to heritable diseases (Barthel et al. [8])		TERC									N
		OBFC1									N
		POT1									N
		RTEL1									N
		TERT	TERT	TERT	TERT		—	—	—		Y
		TP53	TP53	TP53	—	Y	TP53	TP53	—	Y	Y
		NF1	—	—	—		—	—	—		Y
		NF2	—	—	—		—	—	—		Y
		CHK2 (CHEK2)	—	CHEK2	—	Y	—	—	—		Y

Also included is a list of risk mutations related to heritable diseases. Genes identified with VUS that were possibly pathogenic in the GBM cohort are highlighted in bold.

gene most impacted by mutations (34.86%) and shallow or deep deletions (Table S8; Figure S2). EGFR had mutations (26.97%) and CNV gains. FGFR2 (1.53%), JAK2 (1.27%), MYB (1.27%), and ATM (2.04%) had fewer mutations and mostly shallow or deep deletions. Both BRAF (2.54%) and SMO (1.02%) had fewer mutations and mostly low level CNV gains. TP53 (31.55%), PIK3CA (10.18%), and PIK3R1 (10.94%) had relatively high mutations and a mixture of CNV gains and deletions. IDH1 (6.62%), BRCA1 (2.8%), PTCH1 (3.56%), CREBBP (3.56%), MSH6 (3.05%), DAXX (2.29%), TSC2 (2.04%), PPM1D (1.78%), KLK1 (0.51%), and CHEK2 (0.25%) had low rate of mutations and a mixture of CNV low level gains and losses. BRCA1 (2.8%) had low rate of mutations and both CNV low level gains and shallow or deep deletions. The results for the 12 NOTCH, SHH, and WNT pathway genes identified to be impacted in the GBM cohort investigated in the TCGA-GBM and GDC datasets are presented in Table S9 and Figure S3. The WNT pathway genes DICER1 (2.29%), KLF4 (0.25%), and CREBBP (3.56%) had mutations and CNV shallow deletions, as well as low level gains and high level amplifications. TERT (2.80%) and KMT2D (3.05%) had mutations and CNV shallow gains and losses as well as deep deletions. APC (4.58%) and TCF4 (0.76%) had mutations, low level gains, and shallow deletions. The SHH genes, PTCH1 (3.56%), PTCH2 (1.78%), and SMO (1.02%) were impacted by mutations. Whilst the SMO gene had CNV gains, by comparison, the PTCH1 and PTCH2 genes had both CNV gains and losses. NOTCH genes, NOTCH2 (4.07%) and NOTCH1 (0.25%), had mutations and were impacted also by gains and losses in CNV.

3.6. Impact of SNV Burden on Survival in IDH^{WT} GBM Patients. The number of tumour SNVs was prognostic for survival in methylated GBM patients (log rank = 7.63, 95% CI = 6.90–27.10; P value = 0.006, two-sided). Median survival for methylated GBM with ≤ 4 SNVs was 23 months compared to a median survival of 10 months for a tumour with ≥ 5 SNVs (Figure 3; Table S10). For unmethylated GBM patients, the number of tumour SNVs was not prognostic for survival (log rank = 3.393, 95% CI = 9.441–12.559; P value = 0.065).

Median survival was 13 months for unmethylated GBMs with ≤ 4 SNVs, compared to a median survival of 11 months for ≥ 5 SNVs (Figure 4; Table S10). Sample sizes were relatively small in these survival analyses; therefore, the observed trends would need to be confirmed using a larger cohort.

4. Discussion

The mutational landscape of the GBM subtypes in this cohort raises the possibility of new combinations of therapeutic approaches for individual GBM patients. Potentially actionable variation was most often identified in EGFR, PTEN, BRCA1/2, and ATM. These genetic alterations could be targeted by novel approaches with EGFR-targeting antibodies, tyrosine kinase inhibitors, and DNA damage repair inhibitors either singly or in combination. In particular, the BRCA1/2 mutations raise the possibility that DNA damage repair agents may be an option for small numbers of GBM patients in combination with other agents. Administering olaparib PARP (poly (ADP-ribose) polymerase) inhibitor, developed for BRCA1/2 mutated ovarian cancer, in combination with TMZ has shown promising results for treating relapsed glioblastoma patients in a phase I clinical trial (NCT01390571) [44]. However, patient selection to date has not been based on detailed molecular profiling with HTS. In this study's GBM cohort, both IDH^{WT} and IDH^{MUT} GBM had VUS that were predicted to be pathogenic in MSH6 [45–47], CREBBP [48–52], TP53 [17, 47], and TSC2 [36–43, 53]. In particular, MSH6 (MutS homolog 6) is a DNA mismatch-repair protein that has been identified as a putative driver gene in glioma [45, 47]. Similarly, MSH6 may be involved in acquired resistance to alkylating agents [46]. Moreover, CREBBP (CREB binding protein gene/CBP) activates the DNA damage response and repair pathway by acetylating factors involved in base excision repair, nucleotide excision repair, nonhomologous end joining, and double-strand break repair (e.g., PARP-1, H2AX, and NBS1) [49].

4.1. IDH^{WT} Glioblastomas. In IDH^{WT} glioblastomas, SNVs impacted genes in the RTK/Ras/PI(3)K (79%), p53 (61%),

TABLE 4: Summary of the proportion of initial and recurrent of *IDH*-wildtype and *IDH*-mutant glioblastoma patient tumours that had SNVs that could be assigned as potentially clinically actionable.

| Gene | IDH-wildtype | | | | IDH-mutant | | | | Frequency in GBM (Sahm et al.) | Targeted agent (clinical trial) |
| | Initial tumour | | Recurrent tumour | | Initial tumour | | Recurrent tumour | | | |
	N	%	N	%	N	%	N	%	%	
PIK3CA	2/38	5	0/7	0	0/3	0	0/1	0	6.3	mTOR inhibitor; everolimus (NCT02449538); BKM120/everolimus (NCT01470209)
PIK3R1	2/38	5	0/7	0	0/3	0	0/1	0		mTOR inhibitor ABBV-221 (NCT02365662); naratinib
EGFR	6/38	16	1/7	14	0/3	0	0/1	0	34	(NCT01953926); AZD9291 (NCT02465060); EGFR-targeting antibodies, vaccines, TK inhibitors, osimertinib, poziotinib
PDGFRA	2/38	5	0/7	0	0/3	0	0/1	0	11	Dasatinib; nilotinib/Pazopanib (NCT02029001); MGCD516 (NCT02219711)
BRAF	1/38	3	0/7	0	0/3	0	0/1	0		Vemurafenib; MEK inhibitor INC280/BKM120 (NCT01870726); everolimus (NCT02449538); erlotinib, everolimus or dasatinib
PTEN	11/38	29	1/7	14	0/3	0	0/1	0	32	(NCT02233049); GSK2636771 (NCT01458067); BMN673 (NCT02286687); BKM120/everolimus (NCT01470209)
BRCA1	7/38	18	1/7	14	0/3	0	0/1	0		Olaparib
BRCA2	7/38	18	1/7	14	1/3	33	0/1	0		Olaparib
PTCH1	1/38	3	0/7	0	0/3	0	0/1	0		SMO inhibitor, sonidegib and vismodegib
SMO	3/38	8	0/7	0	0/3	0	0/1	0		SMO inhibitor, sonidegib and vismodegib
ATR	3/38	8	0/7	0	0/3	0	0/1	0		ATR inhibitor (BAY1895344)
MSH6	4/38	11	0/7	0	1/3	33	0/1	0		MK-3475 (NCT01876511)
TP53	7/38	18	0/7	0	3/3	100	0/1	0	4.3	
CDKN2A	3/38	8	0/7	0	0/3	0	0/1	0		
RB1	1/38	3	0/7	0	0/3	0	0/1	0		
ATM	6/38	16	1/7	14	0/3	0	0/1	0		

For particular genetic alterations, the proportion of glioblastomas ($n = 47$) with alterations in those genes, as recorded by Sahm et al. [30], is also provided. Also summarised are available and new therapeutic agents currently on trial in clinical studies targeting molecular aberrations.
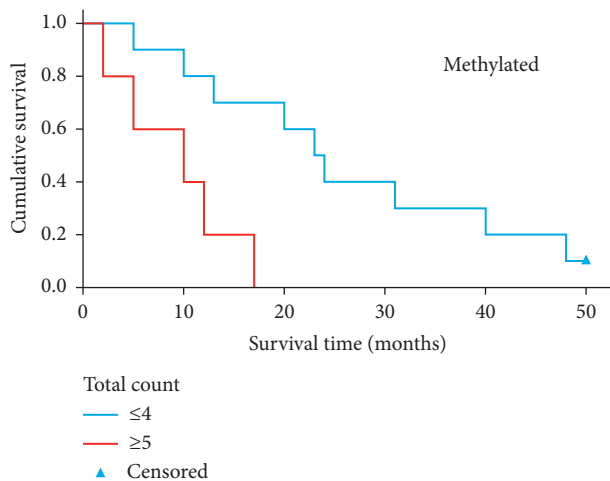
FIGURE 3: Comparison of survival for IDH^{WT} glioblastoma $MGMT$ methylated patients with high versus low total number of tumour SNVs, based on a median split. Kaplan–Meier analysis indicates that IDH^{WT} GBM patients with a greater tumour SNV burden have significantly a shorter overall survival ($P = 0.006$).
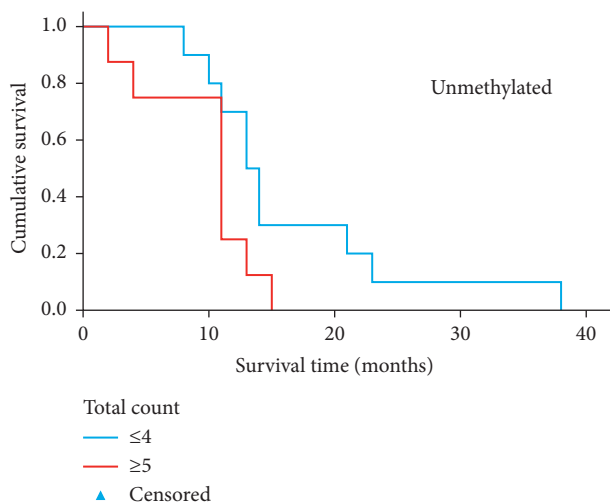

FIGURE 4: Comparison of survival for IDH^{WT} glioblastoma $MGMT$ unmethylated patients with high versus low total number of tumour SNVs, based on a median split. Kaplan–Meier analysis indicates that IDH^{WT} GBM patients with a greater tumour SNV burden have a shorter overall survival; however, this trend was not significant ($P = 0.065$).

WNT (58%), SHH (16%), NOTCH (8%), Rb (5%) and G-protein (5%) pathways. Potentially actionable mutations detected from initial IDH^{WT} tumours included *EGFR, PTEN, BRCA1, BRCA2, ATM,* and *ATR* [54–56]. Therapies for this subtype might include the *EGFR*-targeting antibodies, *EGFR*-targeting vaccines, TK inhibitors, erlotinib, and DNA damage repair inhibitors including olaparib and *ATR* inhibitors. Anti-*EGFR*-targeting antibodies to date have not shown clinical efficacy in GBM although trials are ongoing [57]. Similarly, trials of DNA damage repair inhibitors are underway, and the results are anticipated; however, patients have not been selected for these trials using molecular profiling with HTS.

Interestingly, in this cohort, a high proportion of IDH^{WT} tumours was impacted by *BRCA1* (18%) and *BRCA2* (18%) mutations. This trend was not observed in the TCGA-GBM dataset (2.8%; 2.3%); however, the *IDH* status of patients is not confirmed in most cases [58]. Only one variant from the GBM cohort (*BRCA1*: Ch17: 41246062) was identifiable amongst the TCGA-GBM dataset *BRCA1* ($n = 16$) and *BRCA2* ($n = 39$) variants. The well-known breast cancer specific germline mutations in *BRCA1* (185delAG; Chr17: 43124030–43124031 and 5382insC; Chr17: 43057065) and *BRCA2* (6174delT; Chr13: 32340301) were not amongst the variants identified in either the GBM cohort or the TCGA-GBM cohort. In this GBM cohort, amongst the *BRCA2* variants were confirmed somatic mutations in haemangioblastoma (*BRCA2*: COSM3753648, COSM5019704) [43], which is a rare, benign tumour that typically occurs in the cerebellum [3]. Many IDH^{WT} tumours had alterations impacting WNT [59–63] signalling pathway genes (58%) including *CREBBP*(4), *KLF4*(2) [64, 65], *TERT*(2) [17], and *APC*(3) [66–70]; however, targeting this pathway is currently challenging. Initial IDH^{WT} tumours also showed predicted pathogenic variation in NOTCH (11%) [71] and SHH (13%) pathways [72] including *PTCH1* (*PATCHED-1*) and *SMO* (*Smoothened*) [73–75]. The Hedgehog antagonist GDC-0449 (vismodegib) has been trialled in recurrent GBM (NCT00980343) and childhood brain tumours with varying success to date.

4.2. Recurrent IDH^{WT} Glioblastomas. Interestingly in this cohort, no tumours exhibited a TMZ-induced hypermutated phenotype. Tumours did not have mutations in TERT promoter regions. Kim et al. found that a TMZ-induced hypermutated phenotype was rare in *IDH*-wildtype primary glioblastomas [76]. Acquired resistance in glioma has been attributed to dysregulated pathways (signalling and DNA repair), persistence of cancer stem cell subpopulations, and autophagy mechanisms [77]. In this cohort, only the RTK/Ras/PI(3)K, p53 DNA damage repair, WNT signalling, and G-protein pathways were impacted by genetic alterations and not the SHH, NOTCH, and Rb pathways, despite their association with glioma resistance. Whilst fewer pathways were impacted, intertumour heterogeneity between initial and recurrent *IDH* wildtype tumours was nevertheless observed, similar to previous studies [76, 78]. Indeed, recurrent tumours can diverge to such an extent that they are no longer recognised as lineal descendants of the dominant clone identified initial at diagnosis [78, 79]. Potential signatures of IDH^{WT} recurrent tumour resistance included VUS that were possibly pathogenic in *PTEN*. *PTEN* mutations cause activation of the PI3K/AKT survival pathway and chemoresistance in GBM [80]. Other possible signatures of recurrent tumour resistance in this GBM cohort included CNV gains in the genes (chromosome), *BRCA2* (Chr13), *GNAS* (Guanine nucleotide-binding protein G(s) subunit alpha; Chr20), and *EGFR* (Chr7). Copy number gains are thought to impact driver genes to initiate tumourigenesis. The oncogene *EGFR* is located on chromosome 7, which frequently has CNV gains in *IDH*-wildtype glioblastomas

(~70%) [5, 6]. Gains in the chromosome 20 arm containing *GNAS* are frequently observed in pituitary brain tumours (adenomas) and may exert a mitogenic influence on the WNT signalling pathway via cAMP activation, which may provide a proliferative advantage for resistance [81]. However, *GNAS* has not been identified as a prognostic in dicator implicated in GBM [82]. CNV losses observed in the GBM cohort included *SMARCA4* (Chr19) [47] and *TERT* (Chr5). CNV losses may be concordant with gene expression downregulation [83].

4.3. IDH^{MUT} *Glioblastomas.* Results for *IDH*^{MUT} glioblastomas comprised three initial and one recurrent case only. Pathways impacted by genetic alterations included the RTK/Ras/PI(3)K (66%), p53 (100%), and WNT pathways (33%). Possibly pathogenic VUS identified herein included those co-mutated in both subtypes as well as *KLK1* (kallikrein1). The kallikreins *KLK6, KLK7,* and *KLK9* have been shown to have higher protein levels in Grade IV glioma compared to Grade III tumours and consequently may have utility as prognostic markers for patient survival [84]. All initial *IDH*^{MUT} tumour samples harboured potentially actionable variation in at least one of the genes *TP53, BRCA2,* and *MSH6.* The recurrent tumour had fewer pathways (p53, WNT, and G-protein) impacted by genetic alterations. Matched analysis revealed intertumour heterogeneity. The recurrent *IDH*^{MUT} tumour lacked potentially actionable variation that could be targeted. Given the small sample size for this subtype all trends reported here would need to be confirmed in a larger cohort.

5. Conclusion

Our study reveals that matched initial and recurrent GBM samples harbour potentially actionable variations, and these were most often identified in *EGFR, PTEN, BRCA1/2,* and *ATM.* These genetic alterations could potentially be targeted by novel approaches with EGFR-targeting antibodies, tyrosine kinase inhibitors, and DNA damage repair inhibitors either singly or in combination. This study underlines the need for detailed genetic analysis of GBM patients to identify individuals that might benefit from novel therapeutic approaches that are becoming available in the near future. This information is also important for patient recruitment to clinical trials.

Data Availability

Data are available upon request from the Dept. of Neuropathology, Ruprecht-Karls University of Heidelberg.

Ethical Approval

Ethical approval was given by BRAIN UK and Brain Tumour Bank South West.

Conflicts of Interest

The authors declare that there are no conflicts of interest.

Authors' Contributions

H. P. Ellis and C. E. McInerney contributed equally to this manuscript.

Supplementary Materials

Figure S1: oncoprint plot of mutations and copy number alterations identified in the TCGA-GBM dataset for 8 corresponding genes impacted by CNVs in the GBM cohort. Genes are represented as rows, and individual patients are represented as columns. The right barplot displays the number and type of alterations to each gene, categorised as AMP: high level amplification, GAIN: low level gain, HETLOSS: shallow deletion, HOMDEL: deep deletion, and MUT: SNV mutation event (green). Figure S2: oncoprint plot of mutations and copy number alterations identified in the TCGA-GBM dataset for the 21 corresponding genes impacted by VUS that were possibly pathogenic in the GBM cohort. Genes are represented as rows, and individual patients are represented as columns. The right barplot displays the number and type of alterations to each gene, categorised as AMP: high level amplification, GAIN: low level gain, HETLOSS: shallow deletion, HOMDEL: deep deletion, and MUT: SNV mutation event (green). Figure S3: oncoprint plot of mutations and copy number alterations identified in the TCGA-GBM dataset for 12 WNT/Notch/SHH pathway genes impacted by SNVs in the GBM cohort. Genes are represented as rows, and individual patients are represented as columns. The right barplot displays the number and type of alterations to each gene, categorised as AMP: high level amplification, GAIN: low level gain, HETLOSS: shallow deletion, HOMDEL: deep deletion, and MUT: SNV mutation event (green). Table S1: demographic data for the IDH-wildtype ($n = 38$) and IDH-mutant glioblastomas. Clinical records are for case ID, age, sex, tumour location on the MRI scan, IDH1 R132H hotspot mutation status, patient survival in months, and samples with matched initial and recurrent tumours. Table S2: list of the clinically relevant neuro-oncology genes that were analysed by the HTS-based diagnostic panel used in this study that was developed in Ruprecht Karl-University Heidelberg, Germany (see Sahm et al. [30]). Table S3: summary of the possibly pathogenic VUS identified in initial and recurrent IDH-wildtype and IDH-mutant glioblastoma tumours. The exonic non-synonymous SNVs were predicted to be damaging by both LJB SIFT and FATHMM-MKL tools and had not been recorded by the 1000G database. Descriptive information for tumour, IDH status, genomic position, affected gene and pathway, available dbSNP and COSMIC identifiers,

functional impacts predicted by LJB SIFT and FATHMM-MKL, and a shortened description from InterPro domain are provided. NA; not applicable (see Supplementary Tables Excel File). Table S4: summary of SNVs identified in initial tumours. Descriptive information for tumour, IDH status, genomic position, reference, and alternative variant alleles, affected gene, and pathway, ClinVar significance, functional impacts as predicted by LJB SIFT and FATHMM-MKL and available dbSNP and COSMIC identifiers and InterPro domain description are provided (see Supplementary Tables Excel File). Table S5: summary of SNVs identified in recurrent tumours. Descriptive information for tumour, IDH status, genomic position, reference and alternative variant alleles, affected gene and pathway, ClinVar significance, functional impacts as predicted by LJB SIFT and FATHMM-MKL and available dbSNP and COSMIC identifiers and InterPro domain description are provided (see Supplementary Tables Excel File). Table S6: summary of CNVs identified in initial and recurrent IDH-wildtype glioblastomas. CNV estimation is based on the read depth (%) of the variant (V) compared to a reference control (R; see Methods). Table S7: summary of the SNVs in TCGA-GBM dataset identified for the corresponding genes with VUS that were possibly pathogenic in the GB cohort. Descriptive information for tumour sample, gene, mutation type, amino acid change, genomic position, reference, and alternative variant alleles is provided (see Supplementary Tables Excel File). Table S8: number of cases in TCGA-GBM and GDC mutation datasets affected by mutations in the genes identified to have VUS that are possibly pathogenic in the GB cohort. According to TCGA, a total of 393 cases were tested for somatic mutations. TCGA-GBM comprises a small number of verified ($n = 6$) and ambiguous IDH-mutant cases ($n = 2$; see). Table S9: number of cases in TCGA-GBM and GDC datasets affected by mutations in the WNT, notch, and SHH genes identified to have somatic mutations in the GB cohort. Table S10: mean and median survival time results of the survival analyses to test the impact of SNV burden on overall survival in MGMT methylated and unmethylated IDH-wildtype GBMs. (*Supplementary Materials*)

References

[1] N. G. Burnet, S. J. Jefferies, R. J. Benson, D. P. Hunt, and F. P. Treasure, "Years of life lost (YLL) from cancer is an important measure of population burden- and should be considered when allocating research funds," *British Journal of Cancer*, vol. 92, no. 2, pp. 241–245, 2005.

[2] Q. T. Ostrom, H. Gittleman, J. Xu et al., "CBTRUS statistical report: primary brain and other central nervous system tumors diagnosed in the United States in 2009–2013," *Neuro-oncology*, vol. 18, no. suppl_5, pp. v1–v75, 2016.

[3] D. N. Louis, H. Ohgaki, O. D. Wiestler et al., *WHO Classification of Tumours of the Central Nervous System*, IARC Press, Lyon, France, 4th edition, 2016.

[4] H.-B. Cheng, W. Yue, C. Xie, R.-Y. Zhang, S.-S. Hu, and Z. Wang, "IDH1 mutation is associated with improved overall survival in patients with glioblastoma: a meta-analysis," *Tumor Biology*, vol. 34, no. 6, pp. 3555–3559, 2013.

[5] S. H. Bigner, J. Mark, P. C. Burger et al., "Specific chromosomal abnormalities in malignant human gliomas," *Cancer Research*, vol. 48, no. 2, pp. 405–411, 1988.

[6] M. Ceccarelli, F. P. Barthel, T. M. Malta et al., "Molecular profiling reveals biologically discrete subsets and pathways of progression in diffuse glioma," *Cell*, vol. 164, no. 3, pp. 550–563, 2016.

[7] H. Ohgaki, P. Dessen, B. Jourde et al., "Genetic pathways to glioblastoma," *Cancer Research*, vol. 64, no. 19, pp. 6892–6899, 2004.

[8] F. Barthel, P. Wesseling, and R. G. W. Verhaak, "Reconstructing the molecular life history of gliomas," *Acta Neuropathologica*, vol. 135, no. 5, pp. 649–670, 2018.

[9] L. Dang, D. W. White, S. Gross et al., "Cancer-associated IDH1 mutations produce 2-hydroxyglutarate," *Nature*, vol. 462, no. 7274, pp. 739–744, 2009.

[10] J. R. Prensner and A. M. Chinnaiyan, "Metabolism unhinged: IDH mutations in cancer," *Nature Medicine*, vol. 17, no. 3, pp. 291–293, 2011.

[11] Cancer Genome Atlas Research Network, "Comprehensive genomic characterization defines human glioblastoma genes and core pathways," *Nature*, vol. 455, no. 7216, pp. 1061–1068, 2008.

[12] R. G. W. Verhaak, K. A. Hoadley, E. Purdom et al., "Integrated genomic analysis identifies clinically relevant subtypes of glioblastoma characterized by abnormalities in PDGFRA, IDH1, EGFR, and NF1," *Cancer Cell*, vol. 17, no. 1, pp. 98–110, 2010.

[13] C. W. Brennan, R. G. Verhaak, A. McKenna et al., "The somatic genomic landscape of glioblastoma," *Cell*, vol. 155, no. 2, pp. 462–477, 2013.

[14] H. Suzuki, K. Aoki, K. Chiba et al., "Mutational landscape and clonal architecture in grade II and III gliomas," *Nature Genetics*, vol. 47, no. 5, pp. 458–468, 2015.

[15] Cancer Genome Atlas Research Network, "Comprehensive, integrative genomic analysis of diffuse lower-grade gliomas," *New England Journal of Medicine*, vol. 372, no. 26, pp. 2481–2498, 2015.

[16] D. Speidel, "The role of DNA damage responses in p53 biology," *Archives of Toxicology*, vol. 89, no. 4, pp. 501–517, 2015.

[17] J. H. Lee, J. E. Lee, J. Y. Kahng et al., "Human glioblastoma arises from subventricular zone cells with low-level driver mutations," *Nature*, vol. 560, no. 7717, pp. 243–247, 2018.

[18] B. H. Diplas, X. He, J. A. Brosnan-Cashman et al., "The genomic landscape of TERT promoter wildtype-IDH wildtype glioblastoma," *Nature Communications*, vol. 9, no. 1, p. 2087, 2018.

[19] R. Stupp, W. P. Mason, M. J. Van Den Bent et al., "Radiotherapy plus concomitant and adjuvant temozolomide for glioblastoma," *New England Journal of Medicine*, vol. 352, no. 10, pp. 987–996, 2005.

[20] M. Snuderl, L. Fazlollahi, L. P. Le et al., "Mosaic amplification of multiple receptor tyrosine kinase genes in glioblastoma," *Cancer Cell*, vol. 20, no. 6, pp. 810–817, 2011.

[21] S. C. Mack and P. A. Northcott, "Genomic analysis of childhood brain tumors: methods for genome-wide discovery and precision medicine become mainstream," *Journal of Clinical Oncology*, vol. 35, no. 21, pp. 2346–2354, 2017.

[22] T. Tabone, H. J. Abuhusain, A. K. Nowak, W. N. Erber, and K. L. McDonald, "Clinical outcome of glioma (AGOG) network. Multigene profiling to identify alternative treatment options for glioblastoma: a pilot study," *Journal of Clinical Pathology*, vol. 67, no. 7, pp. 550–555, 2014.

[23] S. H. Ramkissoon, W. L. Bi, S. E. Schumacher et al., "Clinical implementation of integrated whole-genome copy number

and mutation profiling for glioblastoma," *Neuro-oncology*, vol. 17, no. 10, pp. 1344–1355, 2015.

[24] L. Lin, D. Gaut, K. Hu, H. Yan, D. Yin, and H. P. Koeffler, "Dual targeting of glioblastoma multiforme with a proteasome inhibitor (Velcade) and a phosphatidylinositol 3-kinase inhibitor (ZSTK474)," *International Journal of Oncology*, vol. 44, no. 2, pp. 557–562, 2014.

[25] K. Penne, C. Bohlin, S. Schneider, and D. Allen, "Gefitinib (IressaTM, ZD1839) and tyrosine kinase inhibitors: the wave of the future in cancer therapy," *Cancer Nursing*, vol. 28, no. 6, pp. 481–486, 2005.

[26] D. Singh, J. M. Chan, P. Zoppoli et al., "Transforming fusions of FGFR and TACC genes in human glioblastoma," *Science*, vol. 337, no. 6099, pp. 1231–1235, 2012.

[27] D. Rohle, J. Popovici-Muller, N. Palaskas et al., "An inhibitor of mutant IDH1 delays growth and promotes differentiation of glioma cells," *Science*, vol. 340, no. 6132, pp. 626–630, 2013.

[28] R. G. Lerner, S. Grossauer, B. Kadkhodaei et al., "Targeting a Plk1-controlled polarity checkpoint in therapy-resistant glioblastoma-propagating cells," *Cancer Research*, vol. 75, no. 24, pp. 5355–5366, 2015.

[29] R. Roskoski, "Cyclin-dependent protein kinase inhibitors including palbociclib as anticancer drugs," *Pharmacological Research*, vol. 107, pp. 249–275, 2016.

[30] F. Sahm, D. Schrimpf, D. T. W. Jones et al., "Next-generation sequencing in routine brain tumor diagnostics enables an integrated diagnosis and identifies actionable targets," *Acta Neuropathologica*, vol. 131, no. 6, pp. 903–910, 2016.

[31] A. Zacher, K. Kaulich, S. Stepanow et al., "Molecular diagnostics of gliomas using next generation sequencing of a glioma-tailored gene panel," *Brain Pathology*, vol. 27, no. 2, pp. 146–159, 2017.

[32] M. Hummel, S. Bonnin, E. Lowy, and G. Roma, "TEQC: an R package for quality control in target capture experiments," *Bioinformatics*, vol. 27, no. 9, pp. 1316-1317, 2011.

[33] D. Mosen-Ansorena, N. Telleria, S. Veganzones, V. la Orden, M. Maestro, and A. M. Aransay, "seqCNA: an R package for DNA copy number analysis in cancer using high-throughput sequencing," *BMC Genomics*, vol. 15, no. 1, p. 178, 2014.

[34] H. Li, B. Handsaker, A. Wysoker et al., "The sequence alignment/map format and SAMtools," *Bioinformatics*, vol. 25, no. 16, pp. 2078-2079, 2009.

[35] V. Obenchain, M. Lawrence, V. Carey, S. Gogarten, P. Shannon, and M. Morgan, "VariantAnnotation: a bioconductor package for exploration and annotation of genetic variants," *Bioinformatics*, vol. 30, no. 14, pp. 2076–2078, 2014.

[36] X. Chang and K. Wang, "wANNOVAR: annotating genetic variants for personal genomes via the web," *Journal of Medical Genetics*, vol. 49, no. 7, pp. 433–436, 2012.

[37] M. Lek, K. J. Karczewski, E. V. Minikel et al., "Analysis of protein-coding genetic variation in 60,706 humans," *Nature*, vol. 536, no. 7616, pp. 285–291, 2016.

[38] N. Rappaport, S. Fishilevich, R. Nudel et al., "Rational confederation of genes and diseases: NGS interpretation via GeneCards, MalaCards and VarElect," *Biomedical Engineering Online*, vol. 16, no. S1, p. 72, 2017.

[39] H. A. Shihab, M. F. Rogers, J. Gough et al., "An integrative approach to predicting the functional effects of non-coding and coding sequence variation," *Bioinformatics*, vol. 31, no. 10, pp. 1536–1543, 2015.

[40] R. L. Bowman, Q. Wang, A. Carro, R. G. W. Verhaak, and M. Squatrito, "GlioVis data portal for visualization and analysis of brain tumor expression datasets," *Neuro-oncology*, vol. 19, no. 1, pp. 139–141, 2016.

[41] R Core Team, *R: A Language and Environment for Statistical Computing*, R Foundation for Statistical Computing, Vienna, Austria, 2013, http://www.R-project.org/.

[42] M. Giannakis, X. J. Mu, S. A. Shukla et al., "Genomic correlates of immune-cell infiltrates in colorectal carcinoma," *Cell Reports*, vol. 15, no. 4, pp. 857–865, 2016.

[43] G. M. Shankar, A. Taylor-Weiner, N. Lelic et al., "Sporadic hemangioblastomas are characterized by cryptic VHL inactivation," *Acta Neuropathologica Communications*, vol. 2, no. 1, p. 167, 2014.

[44] S. E. R. Halford, G. Cruickshank, L. Dunn et al., "Results of the OPARATIC trial: a phase I dose escalation study of olaparib in combination with temozolomide (TMZ) in patients with relapsed glioblastoma (GBM)," *Journal of Clinical Oncology*, vol. 35, no. 15_suppl, p. 2022, 2017.

[45] A. Liang, B. Zhou, and W. Sun, "Integrated genomic characterization of cancer genes in glioma," *Cancer Cell International*, vol. 17, no. 1, p. 90, 2017.

[46] C. Xie, H. Sheng, N. Zhang, S. Li, X. Wei, and X. Zheng, "Association of MSH6 mutation with glioma susceptibility, drug resistance and progression," *Molecular and Clinical Oncology*, vol. 5, no. 2, pp. 236–240, 2016.

[47] B. E. Johnson, T. Mazor, C. Hong et al., "Mutational analysis reveals the origin and therapy-driven evolution of recurrent glioma," *Science*, vol. 343, no. 6167, pp. 189–193, 2014.

[48] H. M. Chan and N. B. La Thangue, "p300/CBP proteins: HATs for transcriptional bridges and scaffolds," *Journal of Cell Science*, vol. 114, no. 13, pp. 2363–2373, 2001.

[49] I. Dutto, C. Scalera, and E. Prosperi, "CREBBP and p300 lysine acetyl transferases in the DNA damage response," *Cellular and Molecular Life Sciences*, vol. 75, no. 8, pp. 1325–1338, 2018.

[50] Z. Yang, X. Chen, J. Piao, Y. Zhao, H. Yin, and Q. Luo, "Expression of PCAF in brain glioma and its molecular mechanism," *International Journal of Clinical and Experimental Pathology*, vol. 9, no. 3, pp. 3666–3671, 2016.

[51] A. B. Krøigård, M. J. Larsen, A.-V. Lænkholm et al., "Identification of metastasis driver genes by massive parallel sequencing of successive steps of breast cancer progression," *PLoS One*, vol. 13, no. 1, Article ID e0189887, 2018.

[52] M. K. Mallik, "An attempt to understand glioma stem cell biology through centrality analysis of a protein interaction network," *Journal of Theoretical Biology*, vol. 438, pp. 78–91, 2018.

[53] J. A. Chan, H. Zhang, P. S. Roberts et al., "Pathogenesis of tuberous sclerosis subependymal giant cell astrocytomas: biallelic inactivation of TSC1 or TSC2 leads to mTOR activation," *Journal of Neuropathology & Experimental Neurology*, vol. 63, no. 12, pp. 1236–1242, 2004.

[54] D. Burgenske, A. Mladek, and J. Sarkaria, "The selective ATR inhibitor VX-970 enhances the therapeutic effects of standards of care in glioblastoma," *Molecular Cancer Research*, vol. 15, no. 4, 2017.

[55] G. Lombardi, A. Pambuku, L. Bellu et al., "Effectiveness of antiangiogenic drugs in glioblastoma patients: a systematic review and metaanalysis of randomized clinical trials," *Critical Reviews in Oncology/hematology*, vol. 111, pp. 94–102, 2017.

[56] N. N. Laack, E. Galanis, S. K. Anderson et al., "Randomized, placebo-controlled, phase II study of dasatinib with standard chemoradiotherapy for newly diagnosed glioblastoma (GBM), NCCTG N0877 (Alliance)," *Journal of Clinical Oncology*, vol. 33, no. 15_suppl, 2015.

[57] H. K. Gan, D. A. Reardon, A. B. Lassman et al., "Safety, pharmacokinetics, and antitumor response of depatuxizumab

mafodotin as monotherapy or in combination with temozolomide in patients with glioblastoma," *Neuro-oncology*, vol. 20, no. 6, pp. 838–847, 2017.

[58] A. George, S. Kaye, and S. Banerjee, "Delivering widespread BRCA testing and PARP inhibition to patients with ovarian cancer," *Nature Reviews Clinical Oncology*, vol. 14, no. 5, pp. 284–296, 2017.

[59] Y. Lee, J.-K. Lee, S. H. Ahn, J. Lee, and D.-H. Nam, "WNT signaling in glioblastoma and therapeutic opportunities," *Laboratory Investigation*, vol. 96, no. 2, pp. 137–150, 2016.

[60] J. Zhang, K. Huang, Z. Shi et al., "High -catenin/Tcf-4 activity confers glioma progression via direct regulation of AKT2 gene expression," *Neuro-oncology*, vol. 13, no. 6, pp. 600–609, 2011.

[61] H. Zhang, Y. Qi, D. Geng et al., "Expression profile and clinical significance of Wnt signaling in human gliomas," *Oncology Letters*, vol. 15, no. 1, pp. 610–617, 2018.

[62] P. Lu, Y. Wang, X. Liu et al., "Malignant gliomas induce and exploit astrocytic mesenchymal-like transition by activating canonical Wnt/β-catenin signaling," *Medical Oncology*, vol. 33, no. 7, p. 66, 2016.

[63] E. K. Onyido, E. Sweeney, and A. S. Nateri, "Wnt-signalling pathways and microRNAs network in carcinogenesis: experimental and bioinformatics approaches," *Molecular Cancer*, vol. 15, no. 1, p. 56, 2016.

[64] D. T. Dang, J. Pevsner, and V. W. Yang, "The biology of the mammalian Krüppel-like family of transcription factors," *The International Journal of Biochemistry & Cell Biology*, vol. 32, no. 11-12, pp. 1103–1121, 2000.

[65] S. Wang, X. Shi, S. Wei et al., "Krüppel-like factor 4 (KLF4) induces mitochondrial fusion and increases spare respiratory capacity of human glioblastoma cells," *Journal of Biological Chemistry*, vol. 293, no. 17, pp. 6544–6555, 2018.

[66] T. Kantidakis, M. Saponaro, R. Mitter et al., "Mutation of cancer driver MLL2 results in transcription stress and genome instability," *Genes & Development*, vol. 30, no. 4, pp. 408–420, 2016.

[67] Z. Qian, L. Ren, D. Wu et al., "Overexpression of FOXO3A is associated with glioblastoma progression and predicts poor patient prognosis," *International Journal of Cancer*, vol. 140, no. 12, pp. 2792–2804, 2017.

[68] Y.-C. Huang, S.-J. Lin, H.-Y. Shih et al., "Epigenetic regulation of NOTCH1 and NOTCH3 by KMT2A inhibits glioma proliferation," *Oncotarget*, vol. 8, no. 38, p. 63110, 2017.

[69] H. G. Møller, A. P. Rasmussen, H. H. Andersen, K. B. Johnsen, M. Henriksen, and M. Duroux, "A systematic review of microRNA in glioblastoma multiforme: micro-modulators in the mesenchymal mode of migration and invasion," *Molecular Neurobiology*, vol. 47, no. 1, pp. 131–144, 2013.

[70] C. Cilibrasi, G. Riva, G. Romano et al., "Resveratrol impairs glioma stem cells proliferation and motility by modulating the WNT signaling pathway," *PLoS One*, vol. 12, no. 1, Article ID e0169854, 2017.

[71] U. D. Kahlert, M. Cheng, K. Koch et al., "Alterations in cellular metabolome after pharmacological inhibition of Notch in glioblastoma cells," *International Journal of Cancer*, vol. 138, no. 5, pp. 1246–1255, 2016.

[72] N. Takebe, P. J. Harris, R. Q. Warren, and S. P. Ivy, "Targeting cancer stem cells by inhibiting Wnt, Notch, and Hedgehog pathways," *Nature Reviews Clinical Oncology*, vol. 8, no. 2, pp. 97–106, 2011.

[73] X. Li, W. Deng, S. M. Lobo-Ruppert, and J. M. Ruppert, "Gli1 acts through Snail and E-cadherin to promote nuclear signaling by β-catenin," *Oncogene*, vol. 26, no. 31, pp. 4489–4498, 2007.

[74] K. Wang, L. Pan, X. Che, D. Cui, and C. Li, "Gli1 inhibition induces cell-cycle arrest and enhanced apoptosis in brain glioma cell lines," *Journal of Neuro-Oncology*, vol. 98, no. 3, pp. 319–327, 2010.

[75] M. H. Shahi, S. Farheen, M. P. M. Mariyath, and J. S. Castresana, "Potential role of Shh-Gli1-BMI1 signaling pathway nexus in glioma chemoresistance," *Tumor Biology*, vol. 37, no. 11, pp. 15107–15114, 2016.

[76] J. Kim, I.-H. Lee, H. J. Cho et al., "Spatiotemporal evolution of the primary glioblastoma genome," *Cancer Cell*, vol. 28, no. 3, pp. 318–328, 2015.

[77] S. Osuka and E. G. Van Meir, "Overcoming therapeutic resistance in glioblastoma: the way forward," *Journal of Clinical Investigation*, vol. 127, no. 2, pp. 415–426, 2017.

[78] J. Wang, E. Cazzato, E. Ladewig et al., "Clonal evolution of glioblastoma under therapy," *Nature Genetics*, vol. 48, no. 7, pp. 768–776, 2016.

[79] J. M. Findlay, F. Castro-Giner, S. Makino et al., "Differential clonal evolution in oesophageal cancers in response to neo-adjuvant chemotherapy," *Nature Communications*, vol. 7, no. 1, p. 11111, 2016.

[80] J. R. Molina, Y. Hayashi, C. Stephens, and M. M. Georgescu, "Invasive glioblastoma cells acquire stemness and increased Akt activation," *Neoplasia*, vol. 12, no. 6, pp. 453–463, 2010.

[81] W. L. Bi, N. F. Greenwald, S. H. Ramkissoon et al., "Clinical identification of oncogenic drivers and copy-number alterations in pituitary tumors," *Endocrinology*, vol. 158, no. 7, pp. 2284–2291, 2017.

[82] N. El Hindy, N. Lambertz, H. S. Bachmann et al., "Role of the GNAS1 T393C polymorphism in patients with glioblastoma multiforme," *Journal of Clinical Neuroscience*, vol. 18, no. 11, pp. 1495–1499, 2011.

[83] R. Wei, M. Zhao, C. H. Zheng, M. Zhao, and J. Xia, "Concordance between somatic copy number loss and down-regulated expression: a pan-cancer study of cancer predisposition genes," *Scientific Reports*, vol. 6, no. 1, Article ID 37358, 2016.

[84] K. L. Drucker, C. Giannini, P. A. Decker, E. P. Diamandis, and I. A. Scarisbrick, "Prognostic significance of multiple kallikreins in high-grade astrocytoma," *BMC Cancer*, vol. 15, no. 1, p. 565, 2015.